Article

SENP2 negatively regulates cellular antiviral response by deSUMOylating IRF3 and conditioning it for ubiquitination and degradation

Yong Ran[1], Tian-Tian Liu[1], Qian Zhou[1], Shu Li[1], Ai-Ping Mao[1], Ying Li[1], Li-Juan Liu[1], Jin-Ke Cheng[2], and Hong-Bing Shu[1,*]

1 College of Life Sciences, Wuhan University, Wuhan 430072, China
2 Department of Biochemistry and Molecular Cell Biology, School of Medicine, Shanghai Jiao Tong University, Shanghai 200025, China
* Correspondence to: Hong-Bing Shu, E-mail: shuh@whu.edu.cn

Transcription factor IRF3-mediated type I interferon induction is essential for antiviral innate immunity. We identified the deSUMOylating enzyme Sentrin/SUMO-specific protease (SENP) 2 as a negative regulator of virus-triggered IFN-β induction. Overexpression of SENP2 caused IRF3 deSUMOylation, K48-linked ubiquitination, and degradation, whereas depletion of SENP2 had opposite effects. Both the SUMOylation and K48-linked ubiquitination of IRF3 occurred at lysines 70 and 87, and these processes are competitive. The level of virus-triggered IFN-β was markedly up-regulated and viral replication was reduced in SENP2-deficient cells comparing with wild-type controls. Our findings suggest that SENP2 regulates antiviral innate immunity by deSUMOylating IRF3 and conditioning it for ubiquitination and degradation, and provide an example of cross-talk between the ubiquitin and SUMO pathways in innate immunity.

Keywords: SENP2, IRF3, deSUMOylation, ubiquitination, innate immunity

Introduction

The innate immune response is an important mechanism that protects the host from microbial infection by triggering a series of signaling events that lead to induction of type I IFNs (Akira et al., 2006; O'Neill and Bowie, 2010) by PRRs such as the Toll-like receptors (TLRs) and RIG-I-like receptors (RLRs). TLR3 recognizes dsRNA produced during viral replication and then signals IFN induction through TRIF-dependent pathways in immune cells (Blasius and Beutler, 2010). The RLRs, including RIG-I and MDA5, act as cytoplasmic sensors for viral RNAs in most cell types (Akira et al., 2006) through their C-terminal RNA helicase domains, then undergo conformational changes and are recruited to the downstream adaptor protein VISA (also known as MAVS, IPS-1 and Cardif) through CARD domains (Xu et al., 2005; O'Neill and Bowie, 2010). VISA is located at the outermembrane of mitochondria and acts as a central platform for assembly of a complex that mediates both the IRF3 and NF-κB activation pathways after viral infection. VISA-mediated NF-κB activation requires TRAF6 and IKK, and VISA-mediated IRF3 activation needs TRAF3 and TBK1 or IKKε (Fitzgerald et al., 2003; Xu et al., 2005; Oganesyan et al., 2006). Other molecules, such as MITA/STING, GSK3β, WDR5, NLRX1, TRADD, FADD, and RIP1, also participate in or regulate RLR-mediated induction of type I IFNs (Ishikawa and Barber, 2008; Michallet et al., 2008; Moore et al., 2008; Zhong et al., 2008; Lei et al., 2010; Nakhaei et al., 2010; Wang et al., 2010).

Many studies have suggested critical roles for post-translational modifications in regulation of virus-triggered IFN induction. The virus-triggered IFN pathways are heavily regulated by ubiquitination and deubiquitination. The E3 ubiquitin ligases TRIM25 and Riplet/REUL catalyze K63-linked ubiquitination of RIG-I (Gack et al., 2007; Gao et al., 2009), while the ovarian tumor (OTU)-domain-containing deubiquitinating enzymes CYLD and A20 dissociate K63-linked ubiquitin moieties from RIG-I, thereby negatively regulating RIG-I-mediated signaling (Wang et al., 2004; Lin et al., 2006; Friedman et al., 2008). VISA is also ubiquitinated and degraded by the E3 ubiquitin ligases RNF5 and AIP4 (You et al., 2009; Zhong et al., 2010). TRAF3 and TRAF6 are themselves E3 ubiquitin ligases, and regulated by the ubiquitin ligases cIAP1 and cIAP2, and the deubiquitination enzymes OTUB5 (DUBA), OTUB1, and OTUB2 (Kayagaki et al., 2007; Li et al., 2010; Mao et al., 2010). MITA, IKKγ, IRF3, and IκBα are also regulated by ubiquitination and deubiquitination (Zhang et al., 2008; Zhong et al., 2009).

SUMO can function as antagonist of ubiquitin in the regulation of certain substrates. SUMOylation of IκBα causes its resistant to degradation by preventing its ubiquitination (Hay, 2005). On the other hand, SUMO can also act as a signal for the recruitment of E3 ubiquitin ligase, promoting the ubiquitination, and

Received July 7, 2011. Accepted July 14, 2011.

degradation of the modified protein (Cheng et al., 2007). SUMO conjugation is a reversible process in that it can be readily reversed by Sentrin/SUMO-specific proteases (SENPs) (Mukhopadhyay and Dasso, 2007), which belong to the peptidase C48 family. This family of proteases includes SENP1–3 and SENP5–8, which can be divided into three subfamilies on the basis of their sequence homology, cellular location, and substrate specificity. The physiological functions for most SENPs are not well understood. It has been demonstrated that SENP2 is involved in divergent physiological processes by modulating its substrates. For example, SENP2 plays a critical role in the control of adipogenesis by deSUMOylating C/EBPβ and subsequently inhibiting its ubiquitination and degradation (Chung et al., 2010). SENP2 also plays an essential role in development by regulating the p53–Mdm2 pathway (Chiu et al., 2008). However, the functions of SENPs in cellular processes are only at the beginning of being revealed.

In this study, we identified SENP2 as a negative regulator of virus-triggered type I IFN induction and cellular antiviral response. We further found that SENP2 acts by deSUMOylating IRF3 and conditioning it for ubiquitination and degradation. Our study provides the first example of the cross-talk between ubiquitination and SUMOylation in regulation of virus-triggered IFN induction and innate antiviral response.

Results

Identification of SENP2 as a negative regulator of virus-triggered signaling pathway

Type I IFNs play key roles in antiviral innate immune response. However, cells do not express type I IFNs under physiological conditions, while over-production of IFNs upon microbial infection results in autoimmune disorders. To further investigate the regulatory mechanisms of virus-triggered induction of type I IFNs, we screened a protease cDNA array containing 352 clones for proteases that regulate virus-triggered IFN-β promoter activation by reporter assays. These assays identified SENP2 as an inhibitor of Sendai virus (SeV)-triggered activation of the IFN-β promoter. In the same assays, SENP1 and SENP7, two members of the SENP family had less or no effects on SeV-triggered activation of the IFN-β promoter (Figure 1A). Further experiments indicated that overexpression of SENP2 inhibited SeV-triggered activation of the IFN-β promoter in a dose-dependent manner in 293 cells (Figure 1B). Overexpression of SENP2 also inhibited SeV-triggered activation of ISRE (an IRF3-binding motif) in a dose-dependent manner in 293 cells (Figure 1B). The effects of SENP2 on virus-triggered activation of the IFN-β promoter and ISRE are not cell-type-specific because similar results were observed in the human lung epithelial A549 cells (Figure 1C). Consistently, SENP2 (but not SENP1) markedly inhibited SeV-triggered transcription of endogenous *IFNB1* gene and the downstream gene *CCL5* in 293 cells (Figure 1D). A catalytically inert mutant of SENP2, SENP2-C548A (Reverter and Lima, 2006), in which the Cys548 is mutated to Ala, had markedly reduced ability to inhibit SeV-triggered activation of the IFN-β promoter, suggesting the hydrolase isopeptidase activity of SENP2 is important for its full inhibitory activity (Figure 1E). In similar experiments, SENP2 did not inhibit IFN-γ-induced activation of the IRF1 promoter (Figure 1F), suggesting that SENP2 specifically inhibits virus-triggered *IFNB1* gene transcription.

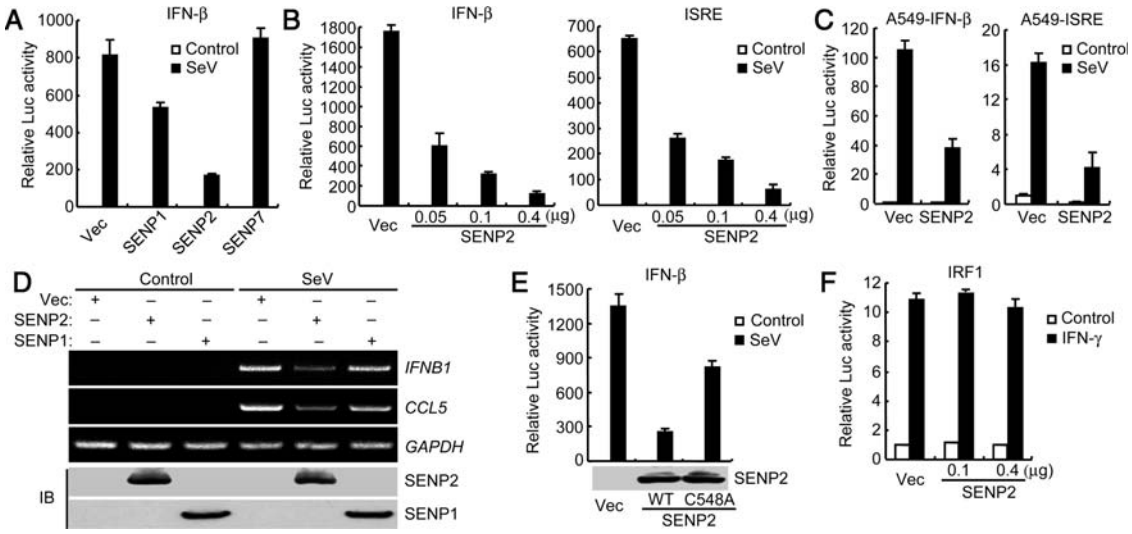

Figure 1 SENP2 inhibits virus-triggered signaling. (**A**) Effects of overexpression of SENP1, 2, and 7 on SeV-triggered IFN-β promoter activation. Human 293 cells (1×10^5) were transfected with the IFN-β reporter (0.1 μg) and the indicated expression (0.1 μg) plasmids. Twenty hours after transfection, cells were infected with SeV or left uninfected for 12 h before luciferase assays were performed. (**B**) Dose-dependent effects of SENP2 on SeV-triggered activation of IFN-β promoter and ISRE. The experiments were similarly performed as in **A**. (**C**) Effects of SENP2 on SeV-triggered activation of the IFN-β promoter and ISRE in A549 cells. The experiments were similarly performed as in **A**. (**D**) Effects of SENP1 and SENP2 on SeV-triggered transcription of *IFNB1* and *CCL5* genes. Human 293 cells (1×10^5) were transfected with expression plasmids for SENP1 and SENP2. Twenty hours later, cells were left uninfected or infected with SeV for 12 h before RT–PCR was performed. (**E**) The effect of SENP2 inactive mutant on SeV-triggered IFN-β promoter activation. The experiments were similarly performed as in **A**. (**F**) The effect of SENP2 on IFN-γ-induced IRF1 promoter activation. Human 293 cells (1×10^5) were transfected with an IRF1 promoter reporter (0.1 μg) and the indicated amounts of SENP2 expression plasmid. Twenty hours after transfection, cells were treated with IFN-γ (100 ng/ml) or left untreated for 12 h before luciferase assays were performed. Data were mean ± SD, $n = 3$. Vec, control vector; Luc, luciferase.

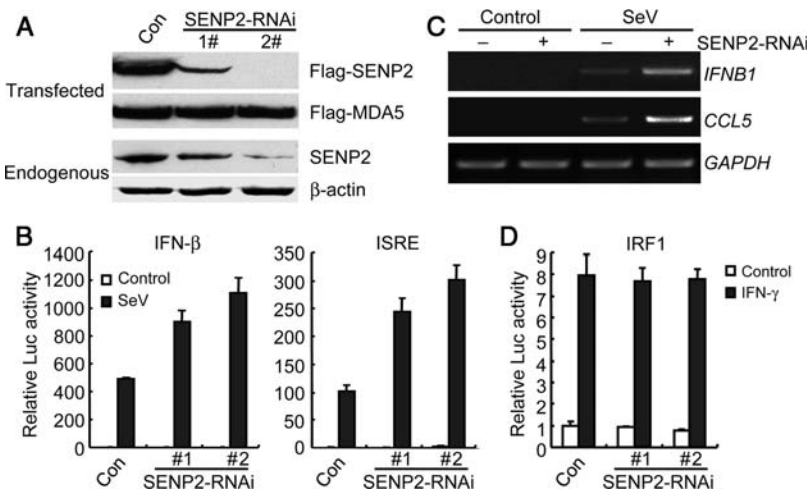

Figure 2 Effects of SENP2 knockdown on virus-triggered signaling. (**A**) Effects of SENP2-RNAi plasmids on the expression of overexpressed or endogenous SENP2. (**B**) Effects of SENP2-RNAi plasmids on SeV-triggered activation of the IFN-β promoter and ISRE. Human 293 cells (1×10^5) were transfected with the indicated reporter (0.1 μg) and RNAi (0.5 μg) plasmids. Thirty-six hours after transfection, cells were left uninfected or infected with SeV for 12 h before reporter assays were performed. (**C**) Effects of SENP2-RNAi plasmids on SeV-triggered transcription of *IFNB1* and *CCL5* genes. Human 293 cells (4×10^5) were transfected with a control or SENP2-RNAi plasmid (#2) (2 μg). Thirty-six hours after transfection, cells were left uninfected or infected with SeV for 12 h before RT–PCR was performed. (**D**) Effects of SENP2-RNAi plasmids on IFN-γ-induced activation of the IRF1 promoter. Human 293 cells (1×10^5) were transfected with an IRF1 promoter reporter (0.1 μg) and the SENP2-RNAi (0.5 μg) plasmid. Thirty-six hours after transfection, cells were treated with IFN-γ (100 ng/ml) or left untreated for 12 h before luciferase reporter assays were performed. Graphs show mean ± SD, $n = 3$. Con, control; Luc, luciferase.

Deficiency of SENP2 potentiates virus-triggered induction of IFN-β and inhibits viral replication

We next investigated the function of endogenous SENP2 in SeV-triggered type I IFN production. We constructed two RNAi plasmids for SENP2, and both of these RNAi plasmids could markedly reduce the expression of transfected and endogenous SENP2 in 293 cells (Figure 2A). In reporter assays, knockdown of SENP2 potentiated SeV-triggered activation of the IFN-β promoter and ISRE (Figure 2B). The degrees of potentiation were correlated with the efficiencies of SENP2 knockdown by these two RNAi plasmids (Figure 2A and B). The SENP2-RNAi#2 plasmid was used for all the following experiments and similar results were obtained with the SENP2-RNAi#1 plasmid. Consistently, the knockdown of SENP2 also potentiated SeV-triggered transcription of endogenous *IFNB1* and *CCL5* genes in 293 cells (Figure 2C). However, the knockdown of SENP2 did not have marked effects on IFN-triggered activation of the IRF1 promoter (Figure 2D), confirming that SENP2 plays a specific role in virus-triggered activation of IRF3 and induction of IFN-β.

Gene knockout of SENP2 in mouse is embryonic lethal (Kang et al., 2010). However, we were able to obtain SENP2-deficient mouse embryonic fibroblasts (MEFs) to further examine the roles of SENP2 in antiviral innate immune response. In reporter assays, SeV-triggered activation of the IFN-β promoter and ISRE was markedly higher in SENP2-deficient cells than their wild-type counterparts (Figure 3A). In addition, activation of the IFN-β promoter induced by cytoplasmic poly(I:C) was also higher in SENP2-deficient cells than the wild-type cells (Figure 3B). Moreover, complementation of SENP2 in SENP2-deficient MEFs markedly impaired SeV- or transfected poly(I:C)-induced activation of the IFN-β promoter (Figure 3C and D). In real-time RT–PCR experiments, we observed that SeV-triggered transcription of the *Ifnb1*, *Ccl5*, and *Isg56* genes were markedly increased in SENP2-deficient MEFs in comparison with the wild-type cells (Figure 3E). The differences of the levels of *Ifnb1*, *Ccl5*, and *Isg56* transcripts between SENP2-deficient and wild-type MEFs were highest (10–100 times) around 12 h after SeV infection (Figure 3E). Consistent with markedly increased expression of the *Ifnb1*, *Ccl5*, and *Isg56* genes, the replication of NDV or SeV was markedly reduced in *Senp2*$^{-/-}$ cells compared with the wild-type cells (Figure 3F and G). Collectively, these results suggest that SENP2 plays a key role in the control of excessive IFN production and cellular antiviral response.

SENP2 regulates virus-triggered signaling at the IRF3 level

Various components are involved in virus-triggered signaling pathways. As shown in Figure 4A, SENP2 inhibited ISRE activation mediated by IRF3 and its upstream components RIG-I, MDA5, VISA, MITA, and TBK1. Consistently, the knockdown of SENP2 potentiated ISRE activation mediated by overexpression of these components (Figure 4B). Similar results were obtained in *Senp2*$^{-/-}$ MEFs (Figure 4C). These results suggest that SENP2 targets IRF3 or a downstream signaling step of IRF3.

SENP2 interacts with and reverses the SUMOylation of IRF3

Previously, it has been demonstrated that mouse IRF3 is modified by SUMOylation at K152 (Kubota et al., 2008). However, this residue of mouse IRF3 is not conserved in human IRF3. Our earlier studies suggest that SENP2 inhibits virus-triggered IFN induction by targeting IRF3 or a downstream signaling step, and the hydrolase isopeptidase activity of SENP2 is important for this process. These findings prompted us to examine whether human IRF3 is modified by SUMOylation and deSUMOylated by SENP2.

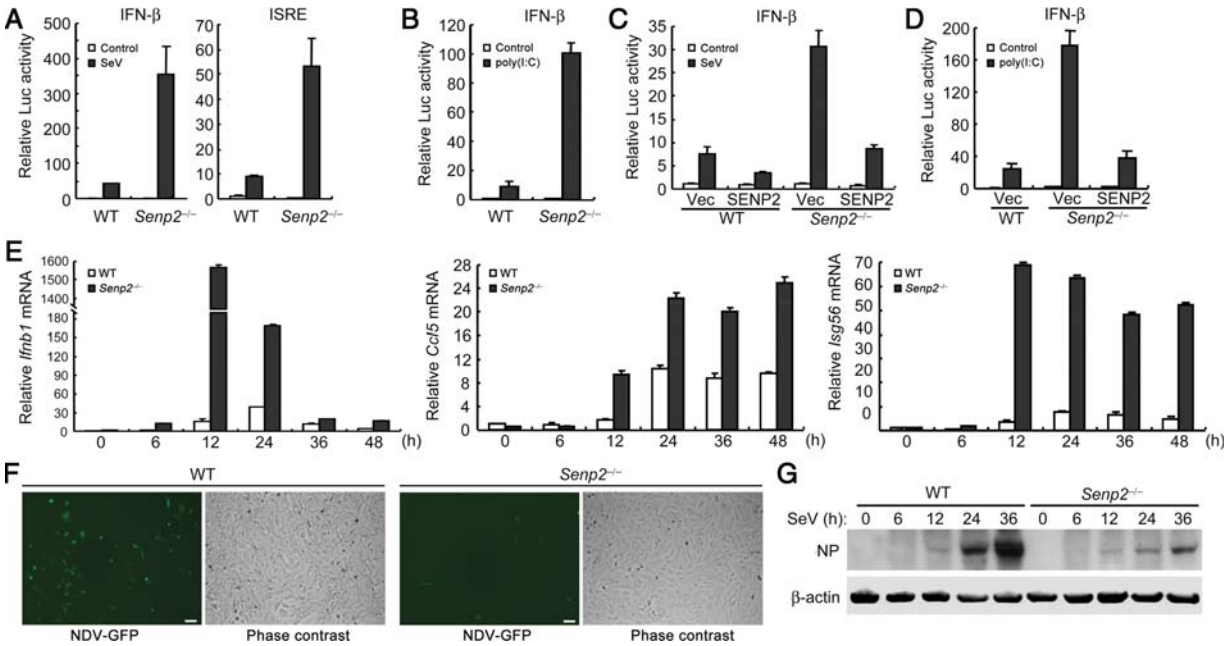

Figure 3 Effects of SENP2 deficiency on virus-triggered signaling. (**A**) Effects of SENP2 deficiency on SeV-triggered activation of the IFN-β promoter and ISRE. *Senp2*$^{-/-}$ and wild-type MEFs (5×10^4) were transfected with the indicated reporter plasmids (0.2 μg). One day after transfection, cells were left uninfected or infected with SeV for 12 h before luciferase assays were performed. (**B**) Effects of SENP2 deficiency on cytoplasmic poly(I:C)-triggered activation of the IFN-β promoter. *Senp2*$^{-/-}$ and wild-type MEFs (5×10^4) were transfected with the IFN-β promoter reporter plasmid (0.2 μg). One day after transfection, cells were retransfected with buffer or poly(I:C) (20 ng) for 20 h before luciferase assays were performed. (**C** and **D**) Reconstitution of SENP2-deficient MEFs with SENP2. *Senp2*$^{-/-}$ and wild-type MEFs (5×10^4) were transfected with the IFN-β promoter reporter (0.1 μg) and empty or SENP2 expression plasmid (2 μg) as indicated. One day after transfection, cells were left untreated or infected with SeV for 12 h (**C**), or cells were retransfected with buffer or poly(I:C) (20 ng) for 20 h (**D**) before luciferase assays were performed. (**E**) SeV-triggered transcription of *Ifnb1*, *Ccl5*, and *Isg56* genes in wild-type and SENP2-deficient MEFs. *Senp2*$^{-/-}$ and wild-type MEFs were infected with SeV for the indicated times before real-time RT–PCR experiments were performed with the indicated primers. (**F** and **G**) NDV and SeV replication in wild-type and *Senp2*$^{-/-}$ MEFs. (**F**) MEFs (5×10^4) were infected by NDV–GFP (MOI = 0.1) for 48 h and imaged by microscopy. Scale bar, 40 μm. (**G**) MEFs were infected with SeV for the indicated times, and the cell lysates were analyzed by immunoblot with an antibody against SeV or β-actin. Data were mean ± SD, $n = 3$. NP, nucleoprotein of SeV; Vec, control vector; Luc, luciferase.

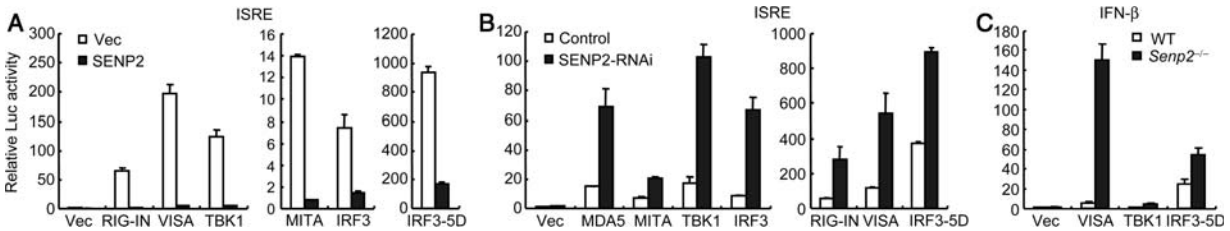

Figure 4 SENP2 targets at or downstream of IRF3. (**A**) Effects of SENP2 on ISRE activation by various signaling components. Human 293 cells (1×10^5) were transfected with an ISRE reporter (0.1 μg), and expression plasmids for SENP2 and the indicated proteins (0.1 μg each). Luciferase assays were performed 24 h after transfection. (**B**) Effects of SENP2 knockdown on ISRE activation by various signaling components. Control or SENP2-RNAi stable cell lines were transfected with ISRE reporter (0.1 μg) and the indicated expression plasmids (0.1 μg each). Luciferase assays were performed 24 h after transfection. (**C**) Effects of SENP2 deficiency on VISA-, TBK1-, and IRF3-mediated IFN-β promoter activation. *Senp2*$^{-/-}$ and wild-type MEFs (5×10^4) were transfected with the IFN-β promoter reporter (0.2 μg) and the indicated expression plasmids (0.5 μg each). Luciferase assays were performed 24 h after transfection. Graphs show mean ± SD, $n = 3$. Vec, control vector; Luc, luciferase.

In human 293 cells, SENP2 was constitutively expressed and viral infection had no marked effect on its expression level (Supplementary Figure S1A). Previously, it has been reported that SENP2 is localized at the nucleoplasmic side of the nuclear pore complex (Mukhopadhyay and Dasso, 2007). Since IRF3 is localized in the cytoplasm under physiological conditions, we determined whether SENP2 is also localized in the cytoplasm. Cell fractionation experiments indicated that SENP2 was localized in both the nucleus and the cytoplasm, and this distribution was not markedly changed following by SeV infection (Supplementary Figure S1B). Immunofluorescent staining experiments indicated that SENP2 was indeed localized at the nuclear pore complex as staining dots, as well as in the cytoplasm, where it at least partially overlapped with IRF3 (Supplementary Figure S1C).

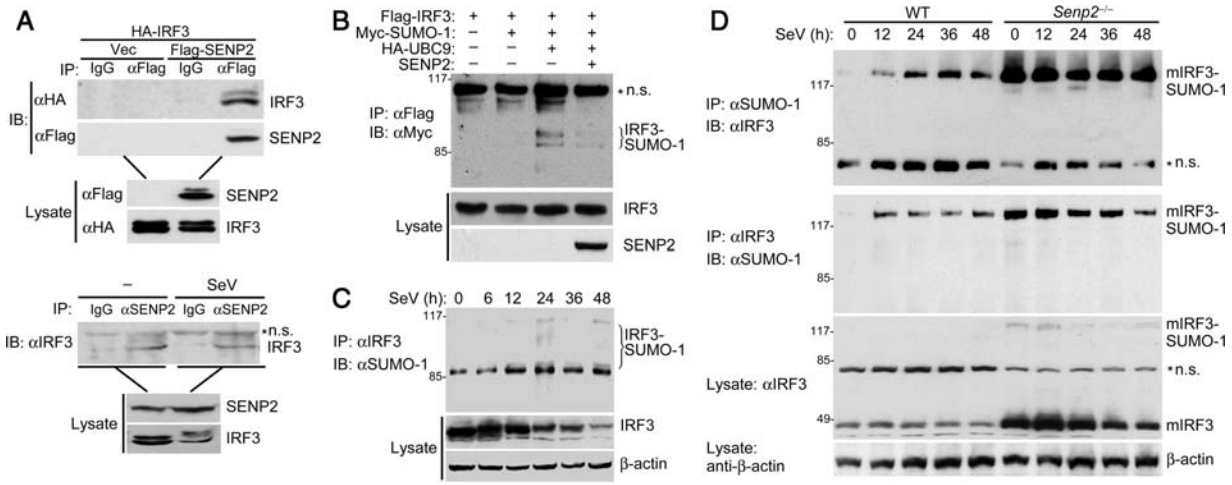

Figure 5 SENP2 mediates deSUMOylation of IRF3. (**A**) Interaction between SENP2 and IRF3 in mammalian overexpression system (upper panel) or untransfected cells (lower panel). Human 293 cells were transfected with the indicated plasmids (upper panel) or infected with SeV for the indicated times (lower panel). Coimmunoprecipitation and immunoblot analysis were performed with the indicated antibodies. (**B**) DeSUMOylation of IRF3 by SENP2. Human 293 cells (2×10^6) were transfected with the indicated plasmids (4 μg each). Coimmunoprecipitation and immunoblot analysis were performed with the indicated antibodies. (**C**) IRF3 SUMOylation in uninfected and viral infected cells. Human 293 cells (1×10^7) were infected with SeV for the indicated times. Coimmunoprecipitation and immunoblot analysis were performed with the indicated antibodies. (**D**) IRF3 SUMOylation in wild-type and SENP2-deficient MEFs. *Senp2*$^{-/-}$ and wild-type MEFs (4×10^6) were infected with SeV for the indicated times. Coimmunoprecipitation and immunoblot analysis were performed with the indicated antibodies. HA, hemagglutinin; mIRF3, mouse IRF3. *n.s., non-specific bands.

In transient transfection and coimmunoprecipitation experiments, SENP2 interacted with IRF3 (Figure 5A, upper panel). The SENP2-C548A mutant also interacted with IRF3 (Supplementary Figure S1D), suggesting that the enzymatic activity is not required for its interaction with IRF3. SENP2 could self-interact, which was also independent of its enzymatic activity (Supplementary Figure S1E). Endogenous coimmunoprecipitation experiments indicated that, SENP2 interacted with IRF3 in untransfected human 293 or MEFs, and this interaction was not affected by SeV infection (Figure 5A, lower panel and Supplementary Figure S1F). These data suggest that SENP2 constitutively interacts with IRF3 in mammalian cells.

We next determined whether IRF3 was modified by SUMOylation. When cotransfected with UBC9 (the SUMO E2-conjugating enzyme), IRF3 was modified by SUMO-1, and the SUMO-1 moiety was removed by overexpression of SENP2 (Figure 5B). In untransfected 293 cells, IRF3 was basally SUMOylated and its SUMOylation was slightly increased following viral infection (Figure 5C). In human 293 cells, the major species of SUMOylated IRF3 was ~90 kDa. Because IRF3 is 47 kDa, and SUMO-1 adds ~20 kDa to the substrates in sodium dodecyl sulfate (SDS)–polyacrylamide gel electrophoresis (PAGE), our results suggest that human IRF3 is probably modified by two SUMO moieties. Similarly, the basal SUMOylation of IRF3 was markedly increased in SENP2-deficient MEFs in comparison with the wild-type cells in uninfected cells (Figure 5D). SeV infection did not further increase the SUMOylation of IRF3 in SENP2-deficient MEFs, probably due to the saturation of IRF3 SUMOylation in these cells (Figure 5D). The molecular weight of the major species of SUMOylated mouse IRF3 was ~120 kDa, suggesting that mouse IRF3 was probably modified by three SUMO-1 moieties. The specificity of the IRF3 SUMOylation in MEFs was further demonstrated by reciprocal immunoprecipitation procedures (Figure 5D). Noticeably, immunoblot analysis with anti-IRF3 also detected a ~80 kDa band in mouse MEFs (Figure 5D). However, this band was not modified IRF3 and represented a non-specific protein recognized by the IRF3 antibody because this band was also detected in IRF3 knockout MEFs (Supplementary Figure S1G). Taken together, these results suggest that both human and mouse IRF3 is modified by SUMO-1 conjugation and deSUMOylated by SENP2.

SENP2 regulates the stability of IRF3

In the transient transfection and coimmunopricipitation experiments, we observed that overexpression of SENP2 caused down-regulation of IRF3 level (Figure 5A), whereas IRF3 level was up-regulated in SENP2-deficient MEFs in comparison with their wild-type counterparts (Figure 5D). These observations suggest that SENP2 directly or indirectly regulates IRF3 stability. We performed additional experiments to confirm these observations. As shown in Figure 6A, overexpression of SENP2 caused down-regulation of IRF3 in a dose-dependent manner, and this was partially blocked by treatment with the proteasome inhibitor MG132 (Figure 6A). In contrast, knockdown of SENP2 in 293 cells markedly increased the level of IRF3, though the increased IRF3 was still degradable following SeV infection (Figure 6B).

IRF3 phosphorylation and dimerization are hallmarks of its activation. We determined the relationship between SENP2-mediated IRF3 degradation and its phosphorylation and dimerization. We found that overexpression of SENP2 did not have an obvious effect on the ratio of dimeric to monomeric IRF3 after SeV infection, though the levels of total and dimeric IRF3 were down-regulated (Figure 6C). Knockdown of SENP2 by RNAi also did not affect the ratio of phosphorylated or dimerized IRF3 to total or monomeric IRF3 after SeV infection, though the levels of

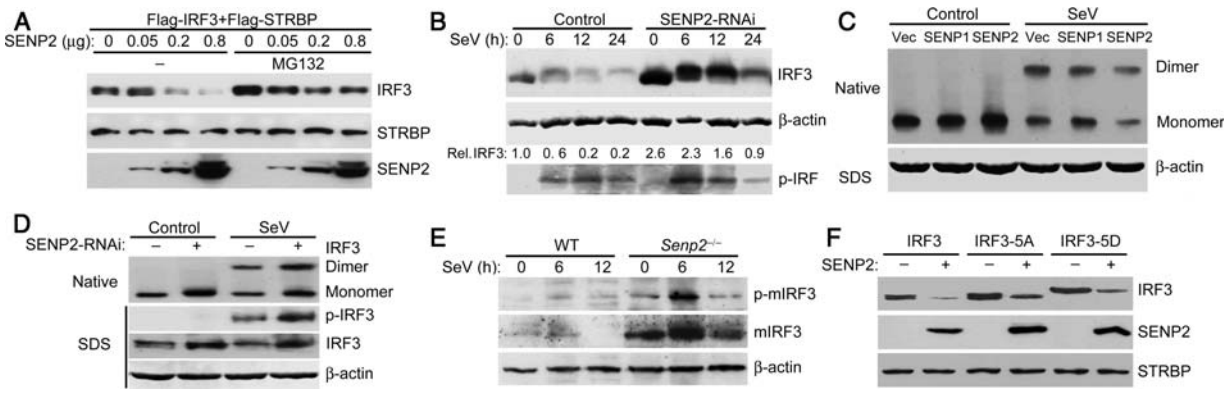

Figure 6 SENP2 regulates the stability of IRF3. (**A**) SENP2 causes IRF3 degradation in a dose-dependent manner. Human 293 cells were transfected with the indicated plasmids for 24 h and left untreated or treated with MG132 for 6 h before analyzed by immunoblots with anti-Flag and anti-SENP2. (**B**) Effects of SENP2 knockdown on IRF3 levels. Control or SENP2-RNAi stable cell lines were infected with SeV for the indicated times and analyzed by immunoblots with the indicated antibodies. The amounts of IRF3 were quantitated using the Bio-Rad Quantity One Program and were normalized to that of β-actin. (**C**) The effect of SENP2 on SeV-triggered dimerization of endogenous IRF3. Human 293 cells were transfected with the indicated plasmids for 24 h, then left uninfected or infected with SeV for 8 h followed by native or SDS–PAGE and immunoblots with anti-IRF3 and anti-β-actin respectively. (**D**) Effects of SENP2 knockdown on SeV-triggered IRF3 phosphorylation and dimerization. Control or SENP2-RNAi stable cell lines were left uninfected or infected with SeV for 8 h. Cell lysates were separated with native or SDS–PAGE and followed by immunoblots with the indicated antibodies. (**E**) IRF3 phosphorylation in wild-type and *Senp2*$^{-/-}$ MEFs. MEFs (4×10^5) were left uninfected or infected with SeV for the indicated times and then analyzed by immunoblots with the indicated antibodies. (**F**) Effects of SENP2 on the levels of wild-type IRF3 and its mutants. Human 293 cells (4×10^5) were transfected with the indicated plasmids for 24 h before analyzed by immunoblots with anti-Flag. mIRF3, mouse IRF3.

total or phosphorylated/dimeric IRF3 increased following SENP2 knockdown (Figure 6B and D). Similar results were observed in SENP2-deficient cells, in which the levels of total and phoshorylated IRF3 were increased following SeV infection (Figure 6E). Overexpression of SENP2 caused down-regulation of wild-type IRF3, as well as IRF3-5A and IRF3-5D, which are inactive or constitutive active IRF3 mutant, respectively (Figure 6F). These results suggest that SENP2-mediated deSUMOylation and degradation of IRF3 and virus-triggered phoshorylation and dimerization of IRF3 are independent events.

SENP2 regulates the ubiquitination of IRF3

It has been suggested that IRF3 stability is regulated by ubiquitination. The ability of SENP2 to regulate IRF3 stability suggests the possibility that SENP2 plays a role in regulating IRF3 ubiquitination. To test this hypothesis, we examined the effect of SENP2 on ubiquitination of endogenous IRF3 in 293 cells. We found that overexpression of SENP2 increased the K48-linked ubiquitination of IRF3 in both uninfected and infected cells (Figure 7A), while decreased the SeV-trigged K63-linked ubiquitination of IRF3 (Supplementary Figure S2A). Knockdown of SENP2 in 293 cells had opposite effects (Figure 7B and Supplementary Figure S2B). Furthermore, K48-linked ubiquitination of IRF3 was decreased in SENP2-deficient MEFs in comparison with their wild-type counterparts, in either uninfected or viral infected cells (Figure 7C). Taken together, these results suggest that SENP2, which mediates deSUMOylation of IRF3, promotes K48-linked ubiquitination and degradation of IRF3 in both uninfected and viral infected cells.

Mapping of SUMOylation and ubiquitination sites of IRF3

Since SENP2-mediated deSUMOylation and K48-linked ubiquitination of IRF3 are correlated, and both SUMOylation and ubiquitination target lysine residues of the substrates, we reasoned that SUMOylation and K48-linked ubiquitination of IRF3 occur at the same lysine residue(s). To test this hypothesis, several potential SUMO conjugating lysines of human IRF3 predicted by the SUMOplot Analysis Program were mutated to arginines. Immunoprecipitation experiments indicated that the SUMOylation of K70R and K87R mutants of IRF3 decreased markedly, whereas double mutation of K70 and K87 abolished the SUMOylation of IRF3, suggesting that these two residues are targeted for SUMOylation (Figure 7D). Interestingly, the K70R/K87R double mutant had markedly reduced ubiquitination level in comparison with the wild-type or each of the two single mutants, suggesting that these two lysine residues of IRF3 are also targeted for ubiquitination (Figure 7E). Previously, it has been demonstrated that K152 of mouse IRF3 is SUMOylated. However, this residue is not conserved in human IRF3. We further investigated the residues of mouse IRF3 targeted for SUMOylation and ubiquitination by mutagenesis. The results indicated that K87 and K152 were two major residues of mouse IRF3 targeted for SUMOylation, because mutation of either of the residues caused a marked loss of a ~90 kDa band that was probably mouse IRF3 modified with two copies of SUMO moieties (Supplementary Figure S2C). In these experiments, a strong SUMOylated band of ~70 kDa was detected with the K152R mutant, suggesting that mutant was still able to be monoSUMOylated at K87 (Supplementary Figure S2C). Interestingly, a ~70 kDa SUMOylated band was not detected with the K87R mutant (Supplementary Figure S2C). The simplest explanation for this observation is that SUMOylation at K87 is a prerequisite for further SUMOylation at K152. Ubiquitination experiments indicated that K87 was one major residue of mouse IRF3 targeted for ubiquitination (Supplementary Figure S2D). These results suggest that K87 is a conserved residue in human and mouse IRF3 that is targeted for both SUMOylation and K48-linked ubiquitination.

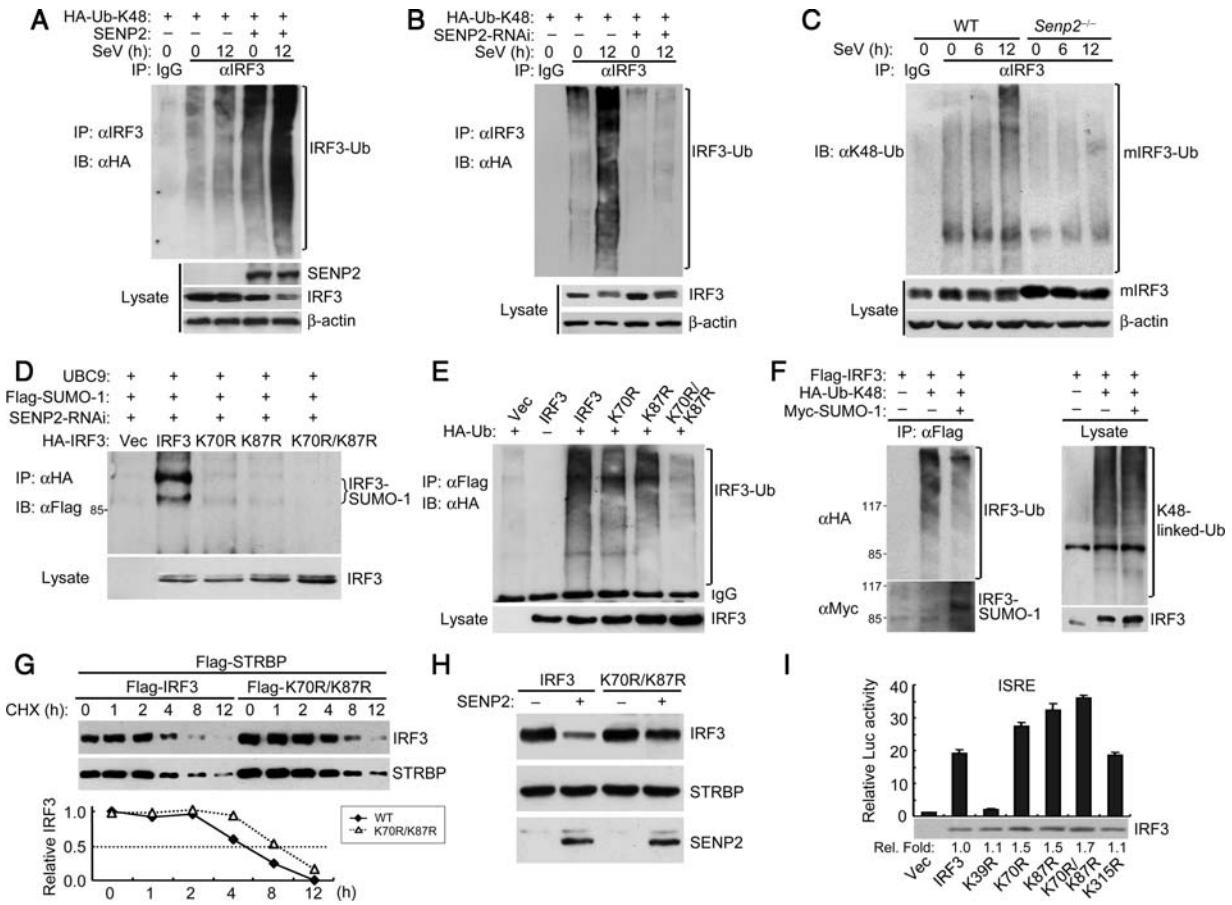

Figure 7 Effects of SENP2 on ubiquitination and degradation of IRF3. (**A** and **B**) Effects of overexpression (**A**) or knockdown (**B**) of SENP2 on K48-linked ubiquitination of IRF3. Human 293 cells (2×10^6) were transfected with SENP2 (10 μg) (**A**) or SENP2-RNAi (10 μg) (**B**) plasmid together with HA-K48-Ub plasmid (0.5 μg). Cells were infected with SeV for 8 h and treated with MG132 for 6 h before coimmunoprecipitation and immunoblot analysis were performed with the indicated antibodies. (**C**) Effects of SENP2 deficiency on K48-linked ubiquitination of IRF3. MEFs (4×10^6) were infected with SeV for the indicated times. Coimmunoprecipitation and immunoblot analysis were performed with the indicated antibodies. (**D**) Mapping of SUMO conjugating sites of IRF3. Human 293 cells (2×10^6) were transfected with the indicated plasmids. Coimmunoprecipitation and immunoblot analysis were performed with the indicated antibodies. (**E**) Mapping of ubiquitin conjugating sites of IRF3. Human 293 cells (2×10^6) were transfected with Flag-tagged IRF3 or its mutants, as well as HA-Ub as indicated. Coimmunoprecipitation and immunoblot analysis were performed with the indicated antibodies. (**F**) Role of SUMOylation on K48-linked ubiquitination of IRF3. Human 293 cells (2×10^6) were transfected as indicated. Coimmunoprecipitation and immunoblot analysis were performed with the indicated antibodies. (**G**) Measurement of the half-life of IRF3 and the K70R/K87R mutant. Human 293 cells (4×10^5) were transfected with the indicated plasmids. Cells were treated with cycloheximide (100 μg/ml) for the indicted times. Cell lysates were analyzed by immunoblot with anti-Flag. The IRF3 and its mutant bands were quantitated using the Bio-Rad Quantity One Program and normalized by levels of STRBP (bottom graph). (**H**) Effects of SENP2 on degradation of IRF3 and the K70R/K87R mutant. Human 293 cells (4×10^5) were transfected with Flag-IRF3 or Flag-IRF3 (K70R/K87R), Flag-STRBP and SENP2 plasmids as indicated. Twenty-four hours after transfection, cell lysates were analyzed by immunoblot with anti-Flag. (**I**) Effects of IRF3 mutants on ISRE activation. Human 293 cells (1×10^5) were transfected with ISRE reporter (0.05 μg) and the indicated IRF3 wild-type or mutant plasmids (0.04 μg). Luciferase assays were performed 24 h after transfection. Cell lysates were analyzed by immunoblots with anti-Flag. Graphs show mean ± SD, $n = 3$. HA, hemagglutinin.

Consistent with these results, increased expression of SUMO-1 caused decreased K48-linked ubiquitination of IRF3 in cotransfection system, indicating that conjugation of the SUMO-1 moiety could prevent IRF3 from K48-linked ubiquitination (Figure 7F). In our experiments, we noted that the K70R/K87R mutant was expressed to a higher level in comparison with the wild-type IRF3 (Figure 7D). Inhibition of protein synthesis with cycloheximide indicated that the half-life of the K70R/K87R mutant was longer (~8 h) than the wild-type IRF3 (~5 h) (Figure 7G). Consistently, the K70R/K87R mutant was resistant to SENP2-mediated degradation (Figure 7H). In reporter assays, the K70R/K87R mutant was more potent in activating ISRE than the wild-type and non-related lysine mutants (Figure 7I). Similar to the wild-type IRF3, the K70R/K87R mutant could be translocated into the nucleus when co-expressed with VISA, an activator of the IRF3 pathway (Supplementary Figure S2E). Collectively, these results suggest that the SUMOylation and K48-linked ubiquitination of IRF3 competitively target the same lysine residues, and SUMOylation of IRF3 regulates its stability but not cellular localization.

Discussion

The host antiviral innate immune response is regulated at distinct levels to ensure proper production of type I IFNs following viral infection. IRF3 is a transcription factor essential for virus-triggered type I IFN induction, which is heavily regulated by post-translational modifications. In this study, we found that the deSUMOylating enzyme SENP2 negatively regulated virus-triggered induction of type I IFNs and cellular antiviral response. We further found that SENP2-mediated deSUMOylation and promoted K48-linked ubiquitination and degradation of IRF3. These findings reveal a delicate regulatory mechanism of cellular antiviral response through cross-talk between SUMOylation and ubiquitination of IRF3.

Our results indicated that overexpression of SENP2-inhibited SeV-triggered IFN-β induction, whereas its knockdown had opposite effect. The negative regulatory role of SENP2 in virus-triggered IFN induction was further validated with SENP2-deficient MEFs. Reporter assays as well as real-time PCR experiments demonstrated that IFN-β induction in SENP2-deficient MEFs was markedly up-regulated in comparison with their wild-type control cells. Consistently, replication of NDV and SeV in SENP2-deficient MEFs was markedly inhibited. We conclude from these results that SENP2 plays an important negative regulatory role in virus-triggered IFN induction and cellular antiviral response.

A series of experiments indicate that SENP2 facilitates IRF3 degradation under physiological conditions. Overexpression of SENP2 caused down-regulation of IRF3, whereas knockdown or knockout of SENP2 markedly increased the amount of IRF3 in uninfected cells. In these experiments, overexpression or depletion of SENP2 did not affect the ratios of phosphorylated/dimeric to monomeric or total IRF3 in viral infected cells, though the amounts of phosphorylated/dimeric IRF3 changed due to the down- or up-regulation of total IRF3. In addition, SENP2 down-regulated wild-type IRF3, as well as its inactive or constitutive active mutants, IRF3-5A and IRF3-5D. These results suggest that SENP2 constitutively facilitates IRF3 degradation independent of its active or inactive state. The reason that SENP2 plays a regulatory role in virus-triggered IFN-β induction is due to its ability to regulate the level of IRF3 available for activation after viral infection.

Our experiments suggest that SENP2 promotes ubiquitination and degradation of IRF3 by mediating its deSUMOylation. Firstly, the overexpression of SENP2 potentiated IRF3 ubiquitination, whereas knockdown of SENP2 decreased IRF3 ubiquitination; secondly, the overexpression of SENP2 increased K48-linked but down-regulated K63-linked ubiquitination of IRF3; thirdly, site-directed mutagenesis indicated that lysine 87 was a residue (conserved in human and mouse IRF3) that was targeted for both SUMOylation and K48-linked ubiquitination, and cotransfection experiments indicated that the two processes were competitive; furthermore, mutation of K70/K87 to alanines increased the ability of human IRF3 to activate ISRE. The simplest explanation for these observations is that IRF3 exists in a constant SUMOylation and deSUMOylation equilibrium under physiological conditions, and the deSUMOylation of IRF3 conditions it for K48-linked ubiquitination and proteasome-dependent degradation.

Our experiments indicated that SENP2-C548A, a catalytically inert mutant, had markedly decreased the ability to inhibit SeV-triggered activation of the IFN-β promoter, suggesting that the hydrolase isopeptidase activity of SENP2 is important for its inhibitory role of IRF3 function. However, this mutant remained partial ability to inhibit SeV-triggered IFN-β induction. One of the explanations for this observation is that this mutant can recruit endogenous wild-type SENP2 to IRF3, which is supported by our observation that SENP2 can self-interact or interact with IRF3 independent of its catalytic activity. It is also possible that SENP2 can at least partially act through a deSUMOylation-independent mechanism, or the SENP2-C548A mutant has remained partial enzymatic activity.

A previous study suggests that mouse IRF3 is SUMOylated at K152, a residue not conserved in human IRF3, and this SUMOylation negatively regulates IRF3 transcriptional activity (Kubota et al., 2008). Our experiments suggest that K87 of mouse IRF3, which is conserved in human IRF3, is also targeted for SUMOylation and ubiquitination. These observations imply that human and mouse cells use a common mechanism to regulate IRF3 stability but may use different mechanisms to regulate IRF3 activity.

Interestingly, while the amount of SUMOylated IRF3 was increased in SENP2-deficient cells, probably due to its resistance to K48-linked ubiquitination and degradation, the amount of un-modified IRF3 was also increased in these cells. There are various possibilities that may account for this observation. For example, the accumulation of SUMOylated IRF3 might send an inhibitory signal to IRF3 ubiquitination and degradation. It is also possible that SENP1 or other SENPs might play a redundant role in deSUMOylating IRF3. In *Senp2*$^{-/-}$ MEFs, SUMOylated IRF3 is increased because of deficiency of SENP2, while SENP1 or other SENPs might deSUMOylate IRF3, leading to increased level of un-modified IRF3 in a dynamic process in these cells. In this context, we have observed that SENP1 could inhibit SeV-triggered activation of the IFN-β promoter, though to a less degree in comparison with SENP2.

Our findings that SENP2 regulates IRF3 level in uninfected cells may provide an important mechanism on how to keep IRF3 in a proper level for first-wave of IFN induction and cellular antiviral response after viral infection. This notion was further supported by our observation that the maximum increase of IFN-β expression in SENP2-deficient cells occurred at the beginning time point at which IFN-β was just induced in wild-type cells in real-time PCR experiments. In addition, our findings provide an explanation on how the steady-state amount of IRF3 is maintained under physiological conditions. Since the newly identified E3 ligase RAUL can degrade IRF3 continuously and effectively under physiological condition (Yu and Hayward, 2010), there should be a signal or modification(s) to protect IRF3 from degradation. Based on our study, the simplest model is that SUMOylation of IRF3 renders it resistant to RAUL-mediated K48-linked ubiquitination and degradation, whereas deSUMOylation of IRF3 by SENP2 sensitizes it for K48-linked ubiquitination and degradation. The dynamic equilibrium between SUMOylation and K48-linked ubiquitination of IRF3 is probably the driving force for maintaining IRF3 at a proper level under

physiological condition and for proper IFN induction upon viral infection. In conclusion, our findings elucidate a previously unknown mechanism for modulating an innate antiviral response by regulating IRF3 stability via SENP2, and provide an example of cross-talk between SUMOylation and ubiquitination pathways in innate immune response.

Materials and methods

Reagents

NEM (Sigma), mouse anti-SUMO-1 (Zymed), rabbit monoclonal anti-K48-linked ubiquitin (Millipore) were purchased from the indicated manufacturers. SeV and NDV–GFP were previously described (Xu et al., 2005; Shi et al., 2010). Mouse anti-IRF3 and SENP2 sera were raised against the recombinant mouse IRF3 and human SENP2 proteins, respectively. *Senp2*$^{-/-}$ and wild-type MEFs were previously described (Kang et al., 2010). The other reagents were described (Lei et al., 2010).

Plasmid constructs

Mammalian expression plasmids for human Flag-tagged SENP1 and SENP2 were constructed by standard molecular biology techniques. Mammalian expression plasmids for Flag-tagged human and mouse IRF3 mutants, and the SENP2-C548A mutant were constructed by site-directed mutagenesis. The other expression plasmids and the reporter plasmids were previously described (Xu et al., 2005; Zhong et al., 2008, 2009).

RNAi constructs

Double-strand oligonucleotides corresponding to the target sequences were cloned into the pSuper.retro RNAi plasmid (Oligoengine). The target sequences for human SENP2 cDNA were as follows: #1: 5′-GCGAATTACTCGAGGAGAT-3′; #2: 5′-GGAC AAACCTATCACATTT-3′. A pSuper.retro RNAi plasmid targeting GFP was used as control for all RNAi-related experiments.

Expression screens

The protease clone array was purchased from Origene. The clones were transfected together with the IFN-β promoter luciferase reporter into 293 cells. One day after transfection, cells were infected with SeV or left uninfected for 12 h. The clones that inhibited SeV-triggered activation of the IFN-β promoter were isolated and confirmed by repeating the reporter assays.

SUMOylation and ubiquitination assays

Cells were lysed with RIPA buffer plus complete protease inhibitors and 20 mM NEM, and lysates were sonicated for 1 min. The lysates were centrifuged at 14000 rpm for 20 min at 4°C. The supernatants were incubated with respective antibodies at 4°C overnight before protein G beads were added for 2 h. The beads were washed with cold PBS plus 0.5 M NaCl for three times followed by an additional wash with PBS. Proteins were separated by 8% SDS–PAGE, followed by immunoblot analysis with the indicated antibodies.

Virus manipulation

Viral infection was performed when cells were 70% confluent. The culture medium was replaced by serum-free Dulbecco's modified Eagle's medium (DMEM), and then SeV or NDV–GFP was added into the medium at various multiplicities of infection (MOI) according to the specific experiments. After 1 h, the medium was removed and the cells were fed with DMEM containing 10% FBS. NDV–GFP replication in MEF cells was visualized by fluorescence microscopy and the SeV replication was detected by specific antibody for nucleoprotein of SeV.

Transfection, reporter assays, coimmunoprecipitation, immunoblot and native PAGE, RT–PCR, and real-time PCR

These experiments were performed as described (Xu et al., 2005; Zhong et al., 2008; Lei et al., 2010).

Supplementary material

Supplementary material is available at *Journal of Molecular Cell Biology* online.

Funding

This work was supported by the grants from the National Natural Science Foundation of China (30921001 and 91029302).

Conflict of interest: none declared.

References

Akira, S., Uematsu, S., and Takeuchi, O. (2006). Pathogen recognition and innate immunity. Cell *124*, 783–801.

Blasius, A.L., and Beutler, B. (2010). Intracellular toll-like receptors. Immunity *32*, 305–315.

Cheng, J., Kang, X., Zhang, S., et al. (2007). SUMO-specific protease 1 is essential for stabilization of HIF1alpha during hypoxia. Cell *131*, 584–595.

Chiu, S.Y., Asai, N., Costantini, F., et al. (2008). SUMO-specific protease 2 is essential for modulating p53-Mdm2 in development of trophoblast stem cell niches and lineages. PLoS Biol. *6*, e310.

Chung, S.S., Ahn, B.Y., Kim, M., et al. (2010). Control of adipogenesis by the SUMO-specific protease SENP2. Mol. Cell. Biol. *30*, 2135–2146.

Fitzgerald, K.A., McWhirter, S.M., Faia, K.L., et al. (2003). IKKepsilon and TBK1 are essential components of the IRF3 signaling pathway. Nat. Immunol. *4*, 491–496.

Friedman, C.S., O'Donnell, M.A., Legarda-Addison, D., et al. (2008). The tumour suppressor CYLD is a negative regulator of RIG-I-mediated antiviral response. EMBO Rep. *9*, 930–936.

Gack, M.U., Shin, Y.C., Joo, C.H., et al. (2007). TRIM25 ring-finger E3 ubiquitin ligase is essential for RIG-I-mediated antiviral activity. Nature *446*, 916–920.

Gao, D., Yang, Y.K., Wang, R.P., et al. (2009). REUL is a novel E3 ubiquitin ligase and stimulator of retinoic-acid-inducible gene-I. PLoS One *4*, e5760.

Hay, R.T. (2005). SUMO: a history of modification. Mol. Cell *18*, 1–12.

Ishikawa, H., and Barber, G.N. (2008). STING is an endoplasmic reticulum adaptor that facilitates innate immune signalling. Nature *455*, 674–678.

Kang, X., Qi, Y., Zuo, Y., et al. (2010). SUMO-specific protease 2 is essential for suppression of polycomb group protein-mediated gene silencing during embryonic development. Mol. Cell *38*, 191–201.

Kayagaki, N., Phung, Q., Chan, S., et al. (2007). DUBA: a deubiquitinase that regulates type I interferon production. Science *318*, 1628–1632.

Kubota, T., Matsuoka, M., Chang, T.H., et al. (2008). Virus infection triggers SUMOylation of IRF3 and IRF7, leading to the negative regulation of type I interferon gene expression. J. Biol. Chem. *283*, 25660–25670.

Lei, C.Q., Zhong, B., Zhang, Y., et al. (2010). Glycogen synthase kinase 3beta regulates IRF3 transcription factor-mediated antiviral response via activation of the kinase TBK1. Immunity *33*, 878–889.

Li, S., Zheng, H., Mao, A.P., et al. (2010). Regulation of virus-triggered signaling by OTUB1- and OTUB2-mediated deubiquitination of TRAF3 and TRAF6. J. Biol. Chem. *285*, 4291–4297.

Lin, R., Yang, L., Nakhaei, P., et al. (2006). Negative regulation of the retinoic acid-inducible gene I-induced antiviral state by the ubiquitin-editing protein A20. J. Biol. Chem. *281*, 2095–2103.

Mao, A.P., Li, S., Zhong, B., et al. (2010). Virus-triggered ubiquitination of TRAF3/6 by cIAP1/2 is essential for induction of interferon-beta (IFN-beta) and cellular antiviral response. J. Biol. Chem. *285*, 9470–9476.

Michallet, M.C., Meylan, E., Ermolaeva, M.A., et al. (2008). TRADD protein is an essential component of the RIG-like helicase antiviral pathway.

Immunity *28*, 651–661.
Moore, C.B., Bergstralh, D.T., Duncan, J.A., et al. (2008). NLRX1 is a regulator of mitochondrial antiviral immunity. Nature *451*, 573–577.
Mukhopadhyay, D., and Dasso, M. (2007). Modification in reverse: the SUMO proteases. Trends Biochem. Sci. *32*, 286–295.
Nakhaei, P., Hiscott, J., and Lin, R. (2010). STING-ing the antiviral pathway. J. Mol. Cell Biol. *2*, 110–112.
O'Neill, L.A., and Bowie, A.G. (2010). Sensing and signaling in antiviral innate immunity. Curr. Biol. *20*, R328–R333.
Oganesyan, G., Saha, S.K., Guo, B., et al. (2006). Critical role of TRAF3 in the Toll-like receptor-dependent and -independent antiviral response. Nature *439*, 208–211.
Reverter, D., and Lima, C.D. (2006). Structural basis for SENP2 protease interactions with SUMO precursors and conjugated substrates. Nat. Struct. Mol. Biol. *13*, 1060–1068.
Shi, H.X., Yang, K., Liu, X., et al. (2010). Positive regulation of interferon regulatory factor 3 activation by Herc5 via ISG15 modification. Mol. Cell. Biol. *30*, 2424–2436.
Wang, Y.Y., Li, L., Han, K.J., et al. (2004). A20 is a potent inhibitor of TLR3- and Sendai virus-induced activation of NF-kappaB and ISRE and IFN-beta promoter. FEBS Lett. *576*, 86–90.
Wang, Y.Y., Liu, L.J., Zhong, B., et al. (2010). WDR5 is essential for assembly of the VISA-associated signaling complex and virus-triggered IRF3 and NF-kappaB activation. Proc. Natl Acad. Sci. USA *107*, 815–820.
Xu, L.G., Wang, Y.Y., Han, K.J., et al. (2005). VISA is an adapter protein required for virus-triggered IFN-beta signaling. Mol. Cell *19*, 727–740.
You, F., Sun, H., Zhou, X., et al. (2009). PCBP2 mediates degradation of the adaptor MAVS via the HECT ubiquitin ligase AIP4. Nat. Immunol. *10*, 1300–1308.
Yu, Y., and Hayward, G.S. (2010). The ubiquitin E3 ligase RAUL negatively regulates type I interferon through ubiquitination of the transcription factors IRF7 and IRF3. Immunity *33*, 863–877.
Zhang, M., Tian, Y., Wang, R.P., et al. (2008). Negative feedback regulation of cellular antiviral signaling by RBCK1-mediated degradation of IRF3. Cell Res. *18*, 1096–1104.
Zhong, B., Yang, Y., Li, S., et al. (2008). The adaptor protein MITA links virus-sensing receptors to IRF3 transcription factor activation. Immunity *29*, 538–550.
Zhong, B., Zhang, L., Lei, C., et al. (2009). The ubiquitin ligase RNF5 regulates antiviral responses by mediating degradation of the adaptor protein MITA. Immunity *30*, 397–407.
Zhong, B., Zhang, Y., Tan, B., et al. (2010). The E3 ubiquitin ligase RNF5 targets virus-induced signaling adaptor for ubiquitination and degradation. J. Immunol. *184*, 6249–6255.